AIChE

A Bi-Order Kinetic Model for Poly(methyl methacrylate) Decomposition in HNO_3 Using Microwave Irradiation

Chun-Chih Lin
Dept. of Natural Biotechnology/Institute of Natural Healing Sciences, Nanhua University, Chung Keng Li, Dalin, Chia-Yi 62248, Taiwan

Gia-Luen Guo
Div. of Chemical Analysis, Institute of Nuclear Energy Research, Longtan 32546, Taiwan

Tsuey-Lin Tsai
Div. of Chemical Analysis, Institute of Nuclear Energy Research, Longtan 32546, Taiwan

DOI 10.1002/aic.11813
Published online June 24, 2009 in Wiley InterScience (www.interscience.wiley.com).

In this study, a novel bi-order model combined with zero- and first-order kinetics was proposed for the decomposition of PMMA (MW = 120,000 g/mol) in concentrated HNO_3 by microwave irradiation. To develop and validate this model, Fourier Transform Infrared spectroscopy, scanning electron microscopy, fractional-life method, the gravimetric analysis and Newton's method were utilized. Rate constants, activation energies, the pre-exponential factors and the weight fractions (Φ) *via main-chain scission for the decomposition at 423–453 K were derived from this model. The zero-order reaction was observed dominant at 423–443 K, while the first-order reaction dominated at 453 K and 473 K. The digestion efficiency increased as HNO_3 was increased to >3 mL at 423 K–443 K. At 473 K, the digestion was almost 100% when HNO_3 volume was >3 mL. The estimated Φ values increased with HNO_3 volume at 423 and 443 K, but varied insignificantly at 453 and 473 K.* © 2009 American Institute of Chemical Engineers *AIChE J,* 55: 2150–2158, 2009

Keywords: reaction kinetics, mathematical modeling, microwave digestion, degradation, polymer properties

Introduction

Poly(methyl methacrylate) (PMMA; Figure 1), regarded as a sustainable resource, is a thermoplastics extensively applied to a variety of fields, e.g., nanotechnology,[1–3] microelectronics,[4] automobile industry,[5] dentistry,[6] network communications,[7] battery engineering,[8–12] and articles of daily use.[13] There were ~327,000 tons of PMMA consumed in year 2003 in Western Europe alone.[14] An increase of ~3.2% in global demand was predicted by 2008,[15] which will result in a large amount of waste PMMA being generated by the various industries. As a result, because of resource and environmental concerns, it is imperative that waste PMMA is recycled. An ideal way to recycle PMMA is by regenerating the monomers [methyl methacrylate (MMA)] from waste PMMA followed by their repolymerization, especially when

Correspondence concerning this article should be addressed to C.-C. Lin at cclin@mail.nhu.edu.tw

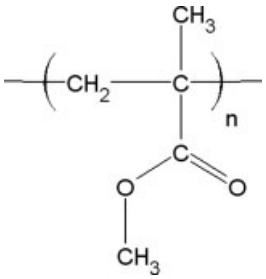

Figure 1. Molecular structure of poly(methyl methacrylate).

the PMMA is mixed with additives, fillers, and dyes.[16] The MMA itself is also a chemical feedstock applied extensively to adhesive formulations, waterborne coatings, and corrosion casts of anatomical organs, which currently costs more than 2 USD/kg.[17]

The decomposition of pure PMMA and PMMA composites by pyrolysis, photochemical reaction, oxidation, high-temperature heating, and mechanical stressing has been intensively investigated.[18–20] Compared with condensation polymers [e.g., poly(ethylene terephthalate)], addition polymers, such as PMMA, are not easily recycled to their monomers by simple chemical methods.[21] Instead, the decomposition of PMMA by thermal degradation has been reported to be feasible and economic for MMA feedstock recycling as investigated recently.[22–26] During degradation, the behavior of polymers depends distinctively on molecular weight, temperature, and gas atmosphere.[27,28] The decomposition of polymers often requires high temperatures and pressures as well as a long reaction time to take place. As a result, microwave digestion has been used as a powerful and versatile method over the last few decades.

Compared with conventional pyrolysis, sample digestion by microwave irradiation has several advantages, such as significantly reducing the time required for pretreatment, minimizing contamination, and sample-loss, as well as providing excellent temperature control. It also provides high decomposition efficiency and precise decomposition monitoring for environmental,[29] material,[30–32] and biological samples.[33,34] Generally, larger amounts of digestion reagents, longer digestion time, or higher digestion temperatures can increase the digestion efficiency. However, the decomposition of the polymer matrix by a specific method is seldom quantitatively evaluated. Therefore, a systematical database of decomposition kinetics would be useful in choosing digestion recipes.

The characterization of the digested sample is the main difficulty in studying kinetics, particularly when the species concentration is one of the kinetic indicators. Thus, another suitable indicator for the digestion is required to probe the kinetics. When digestion is complete, most of the long-chain molecules can be converted into small volatile molecules by fragmentation and removed by further heating. Accordingly, the weight loss method is suitable to investigate the kinetics of microwave digestion in a closed vessel. The decomposition of PMMA occurs successively by initial scission, depropagation reaction, and further degradation into volatile molecules.[35] There are at least two mechanisms validated to date for the initial scission of PMMA. In the initial scission, both the C—C main-chain (backbone) scissions and the side-chain (hemolytic) scissions of the methoxycarbonyl groups are involved, however, the former is dominant in decomposing PMMA into MMA as the major product.[1,36] In addition, CO, CO_2, CH_3OH, CH_4, and char are produced in the elimination of the methoxycarbonyl side groups.[37] In most previous studies, the decomposition of PMMA was investigated as a first order reaction.[1,35,38,39] Other reaction orders that ranged from 1.0 to 1.3 were recently reported.[22,28] Furthermore, depending on the decomposition method and conditions used, different activation energies and Arrhenius constants were also obtained.[1,35,38,39] However, the decomposition behavior and relative kinetics for PMMA by microwave digestion in acid solution in a closed vessel was rarely examined, in which considerable endogenous pressure also exists. Additionally, at high temperatures, the products may be different from those at low temperatures, which may thus lead to different prediction for the reaction kinetics. Most previous studies treated PMMA decomposition as a single order reaction, however, noninteger reaction order may indicate that concurrent reactions are involved. Therefore, in this study, we aimed to provide not only an economical method for recycling PMMA but also to investigate the kinetics and behavior for the decomposition of PMMA (MW = 120,000 g/mol) by microwave/HNO_3 digestion. The related parameters including reaction order, rate constant, and activation energy were also deduced. At the same time, the effect of the amount of HNO_3 on the digestion efficiency of PMMA was explored as well in this work.

Experimental

Reagents and equipments

Reagent-grade poly(methyl methacrylate) obtained from Sigma-Aldrich Co. was in the form of solid powder. Its average molecular weight was 120,000 g/mol. The concentrated HNO_3 (69–70%) was also reagent-grade and supplied by Mallinckrodt Baker, Inc. An electronic balance (Model-AT201; Mettler-Toledo, Inc., Switerland) was used to precisely measure the weight of the samples. The microwave apparatus (MARS 5; CEM, Matthews, NC, USA) was composed of a power device with a selectable output of 0–1200 W (at 2.45 GHz), a Teflon-coated cavity, a computer with programmable settings, a turntable-rotating system for homogeneous heating, and a 14-position sample carousel. A sensor (ESP-1500 Plus) was connected to the control vessel to monitor the pressure, which was set at 2.41×10^6 Pa as the maximum. As the pressure in the vessel exceeded the limit, the microwave oven was automatically shut off. When the endogenous pressure decreased, the microwave oven rebooted. An optical fiber was used to monitor the digestion temperature. The sample was mixed with HNO_3 and digested at various temperatures in a 100 mL double-walled vessel (HP-500 Plus), which comprised a Teflon PFA cover, a chemically resistant inner shell, and an Ultem polyetherimide outer shell. On the vessel, a cap (Autovent Plus) was used to

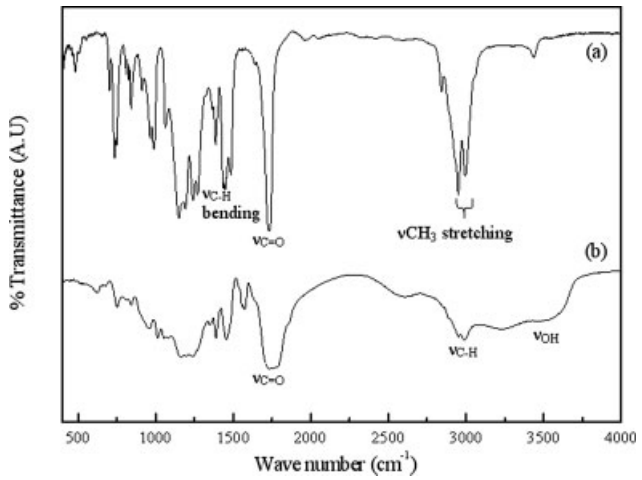

Figure 2. FTIR spectra of virgin PMMA (MW = 120,000 g/mol; dissolved in CH_2Cl_2) (a) before and (b) after microwave/HNO_3 digestion at 453 K.

vent the excessive pressure as well as to avoid the loss of sample and volatile analytes.

Sample treatment for Fourier transform infrared spectroscopy

After decomposition, the sample was completely dried and formed as pellets with KBr. In the control group, pure PMMA was directly dissolved with CH_2Cl_2, pipetted onto a KBr disk, and further baked at 60°C. The digested PMMA and the control samples were then analyzed using an Fourier transform infrared (FTIR) spectrometer (Nicolet Avatar 320; Madison Instruments, Inc., Wisconsin, USA) with 1 cm^{-1} of resolution. All films were thin enough to obey the Beer-Lambert law in this study. The residues of PMMA digested at 453 K were also examined.

Sample treatment for scanning electron microscopy

The digested PMMA solution was diluted 500-fold by dissolving 20 μL of the solution in 10 mL of HNO_3. An aliquot of 2 μL diluted solution was coated on a 0.8 cm $\times$ 0.8 cm silicon wafer using a spin coater (KW-4A; Structure Probe, Inc., USA). After the sample was dried at 60°C, it was coated with gold in the coating chamber for 110 s and then observed using a scanning electron microscope (SEM) (JOEL-JSM-6500F). The size distribution of the PMMA was analyzed using IRCON® software.

Determination of the efficiency on PMMA decomposition

The gravimetric method was utilized to investigate the effects of digestion temperature, digestion time, and HNO_3 volume on the kinetics of PMMA decomposition during microwave/HNO_3 digestion. The digestion efficiency (ξ) described in Eq. 1 was determined by measuring the weight difference of the entirely dried solid sample before and after digestion. The total sample weight before digestion and the remaining weight after digestion were denoted with ω_t and ω_r respectively.

$$\xi(\%) = 100(\omega_t - \omega_r)/\omega_t \quad (1)$$

An aliquot of 0.1 g PMMA and 3 mL of concentrated HNO_3 were added into the reaction vessel and digested under various target temperatures (423, 433, 443, 453, and 473 K) at a constant heating rate to investigate the effect of temperature on digestion efficiency. To examine the effect of HNO_3 on digestion efficiency, the aforementioned procedures were followed except that the amount of concentrated HNO_3 was modified to 2–7 mL.

The PMMA powder was either adhered to the inner wall of the vessel or suspended on the surface of the HNO_3 solution before digestion. When the PMMA was fully decomposed, it was totally dissolved; otherwise, brown solid aggregates would be observed. During microwave/HNO_3 digestion, the color of PMMA powder changed from white to brown and eventually became transparent. To estimate the amount of solid residue, the cooled digested product was transferred to a 20 mL beaker, evaporated on a hot plate to complete dryness, and then weighed with the electronic balance.

Results and Discussion

Figure 2 illustrates the typical FTIR spectra of the PMMA before and after microwave/HNO_3 digestion. Compared with other pyrolysis reactions,[1,40–42] the decomposition by microwave/HNO_3 digestion in closed vessel was found to be able to occur at lower temperature (10 K higher than the melting point of PMMA). This saved more energy than the traditional decomposition methods. The absorbances for aliphatic C—H (SP^3), C=O, and —CH_3 groups were pronounced before PMMA was decomposed as presented in Figure 2a. Absorption arising from C—H stretching of the methyl groups appeared in the region of 3200–2700 cm^{-1}. Numerous saturated hydrocarbons containing methyl groups resulted in asymmetrical and symmetrical stretching of C—H bonding in the methyl group, which corresponded to two distinct peaks at 3000 and 2954 cm^{-1}, respectively. The peak in the region of 1742–1720 cm^{-1} denoted a C=O double bond stretching vibration of the saturated aliphatic esters.[43] The Asymmetrical bending vibration ($\delta_{as}CH_3$) occurred near 1450 cm^{-1}, while the symmetrical bending vibration (δ_sCH_3) appeared near 1387 cm^{-1}.

After microwave digestion (453 K) took place with HNO_3, the broad band of $OH_{stretch}$ in the carboxylic acid group arose in the 3610–3200 cm^{-1} (ν_{OH}) region as shown in Figure 2b. This suggested that the PMMA polymer became hydrophilic after hydrolysis during digestion. Moreover, the absorption of the carbonyl group ($\nu_{C=O}$; stretching of carboxylic acid group) near 1730–1784 cm^{-1} became broadened. This was due to the formation of OH groups by acid hydrolysis. Several broadened peaks which appeared in the 900–1500 cm^{-1} region after digestion denoted the peaks of PMMA branches. This indicated that the dominant products were volatile monomers accompanied with several low-molecular-weight molecules. Compounds with carbonyl groups (e.g., formaldehyde, acetone, and methyl pyruvate) may arise by the oxidation of MMA during PMMA

Table 1. Average Particle Size of PMMA (MW = 120,000 g/mol) after Microwave Digestion at Various Temperatures

Digestion temperature (K)	Mean ± SD* (nm)
Control group†	33.40 ± 14.84
443	26.70 ± 10.94
453	19.02 ± 7.31
463	12.73 ± 6.73
473	9.65 ± 2.70

*Standard deviation of the particle size.
†The acid was removed before baking for sample pretreatment.

decomposition at high temperature.[3,44] Hydrophilic compounds with carboxylic acid groups may also be obtained by acid hydrolysis of transition products during digestion. Furthermore, according to the absorption of C=O and OH groups in the FTIR spectra and the results of our previous study using GC-MS analysis,[45] HCOOH was produced during PMMA decomposition. However, it was arduous to identify whether the fragmented functional groups in the decomposition originated from PMMA or MMA.

The particle size of PMMA revealed a Gaussian distribution and varied with the digestion temperature (Table 1). In the range of 423–473 K, the PMMA particle size declined with increasing temperature, which also expanded the surface area of the materials. In addition, the relative standard deviation is useful in estimating particle size dispersity of the decomposed products after microwave digestion. According to the standard deviations, the range of size distribution narrowed with increasing temperature. Furthermore, the uncertainty in the mean particle size decreased as the digestion temperature increased. The decomposition was generally in agreement with the process of depolymerization, in which small molecule products such as monomers and radicals were produced.[44]

Figure 3 reveals the effect of digestion temperature on the digestion efficiency for PMMA by microwave/HNO_3 digestion. When the temperature increased, the pressure endogenously generated in the closed vessel also dependently increased. The endogenous pressure resulted primarily from the evaporation of HNO_3 and partly from volatile products (e.g., MMA, H_2O, CO, CO_2, and trace of volatile organic compounds). The average translational kinetic energy of the volatile molecules also increased with temperature, which further enhanced the endogenous pressure. This was in agreement with the kinetic-molecular theory of gases[46] and the van de Waals equation.[47] No apparent effect was observed on the digestion efficiency for PMMA at 423 K.

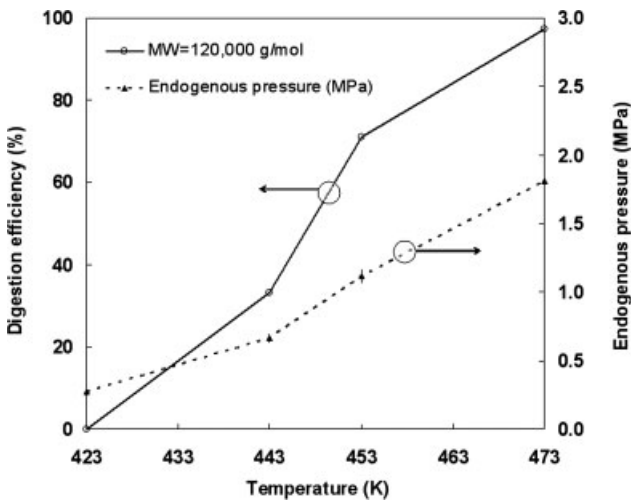

Figure 3. Variation of digestion efficiency with temperature and endogenous pressure.

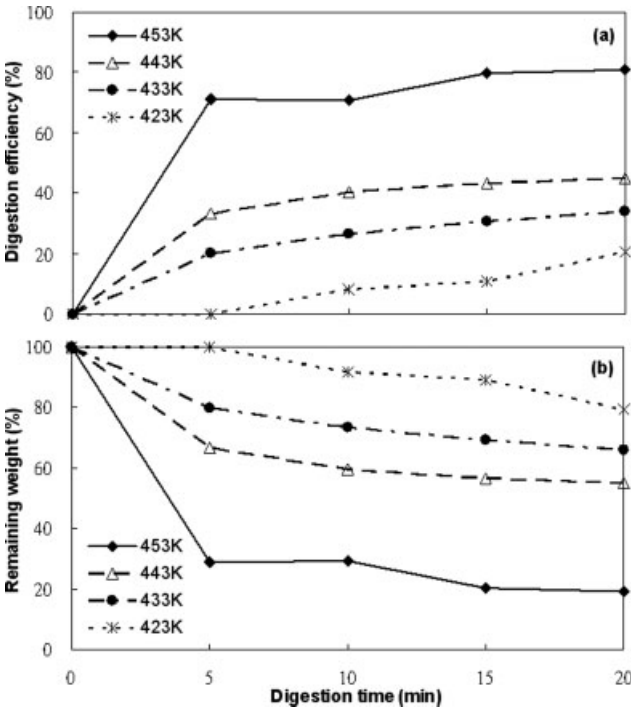

Figure 4. Variation of digestion efficiency as a function of digestion time with different digestion temperatures in 3 mL of nitric acid.

Figure 4a illustrates the variation of digestion efficiency with digestion time at various digestion temperatures. At the same temperature, the digestion efficiency for PMMA increased with digestion time. Furthermore, at the same digestion time, the digestion efficiency also increased with digestion temperature. These results indicated that the decomposition of PMMA by microwave/HNO_3 digestion was a time-dependent reaction. The remaining weight of PMMA varied apparently with digestion time at various heating temperatures as shown in Figure 4b. At the lowest digestion temperature (423 K), the weight loss rates of PMMA appeared to proceed following zero-order kinetics. The coefficient of determination (R^2) of the results obtained by linear regression was 0.916. When the digestion temperature increased to 433 K, the reaction started to diverge from the zero-order kinetics because the coefficient of determination (R^2) of the linear regression line was only 0.848.

As the digestion temperature increased to 443 K, most of the weight loss of PMMA intensively occurred rapidly within 10 min, after which its speed slowly declined. To obtain a preliminary estimate of the reaction order, the fractional-life (τ) method[48] was utilized. By plotting logτ versus

Table 2. Kinetic and Statistical Parameters for PMMA Decomposition in 3 mL of Concentrated HNO_3 Using Microwave Irradiation

Digestion temperature (K)	Mass fraction, Φ (g/g)	Rate constant, k_0 (g/min)	Rate constant, k_1 (min^{-1})
453	0.63	1.15×10^{-3}	1.00
443	0.30	1.10×10^{-3}	0.560
433	0.15	1.08×10^{-3}	0.250
423	5.0×10^{-3}	9.90×10^{-4}	0.102

original weight in a logarithm scale, the reaction order at this temperature was determined from the slope of the linear regression line. The reaction order was 2.57 ($R^2 = 0.982$), which was estimated by defining the fractional life as the time period needed for the original weight of PMMA to decrease to 85%. This suggested that the order of reaction was probably not an integer and the decomposition should involve two simultaneous reactions with different orders.[49]

At a higher temperature, 453 K, the remaining weight of PMMA dropped rapidly within 5 min. Using fractional-life method and defining the fractional life as the time period for the original weight of PMMA to decrease to 85%, the reaction order was determined to be 2.15 with $R^2 = 0.997$. This indicated that the reaction probably proceeded with two concurrent mechanisms with different reaction orders, and the estimated order (2.15) should be a pseudo order.[48] Furthermore, according to the results of FTIR and SEM characterization for the digested compounds of PMMA as well as the digested products reported in literature,[39,44,50] the decomposition of PMMA should involve side-chain and main-chain scissions. In the side-chain scissions, free radicals such as $\cdot CH_3$, $\cdot OCH_3$ and $\cdot COOCH_3$ were possibly generated first,[3] which were further decomposed into small volatile molecules (e.g., CO, CO_2, CH_4 and CH_3OH). On the other hand, the MMA monomers were produced via the main-chain scissions. Consequently, the decomposition of PMMA was proposed as a bi-order reaction involving main-chain and side-chain scissions. The reaction rate (γ) was then developed, as shown in Eq. 2, to achieve a better fit for the decomposition of PMMA:

$$\gamma = -\frac{d\omega}{dt} = \gamma_0 + \gamma_1 = k_0\omega^x + k_1\omega^y \tag{2}$$

where ω and t respectively denoted the weight of PMMA and the digestion time, respectively. Moreover, γ_0 and γ_1 symbolized the rates of PMMA decomposition for side-chain and main-chain scissions, while k_0 and k_1 denoted the rate constants for the two types of scissions, respectively. The superscript letters, x and y, were integers, which represented the reaction order for side-chain and main-chain scissions, respectively. In the main-chain scission, the dominant products were mainly MMA monomers, and its kinetics was generally considered as a first-order reaction.[35,38,39] On the other hand, the side-chain scission (e.g., homolytic scission of methoxycarbonyl side groups) produced low-molecular-weight compounds, which was usually regarded as a zero-order reaction.[1,43,51] Accordingly, a combination of zero- and first-order kinetics was hypothesized for the decomposition of PMMA by microwave irradiation in a fixed amount of HNO_3 (3 mL). The orders, x and y, in Eq. 2 were then replaced by 0 and 1 respectively to obtain Eq. 3.

$$\gamma = -\frac{d\omega}{dt} = \gamma_0 + \gamma_1 = k_0 + k_1\omega \tag{3}$$

Furthermore, the relationship between the remaining weight (ω_0, ω_1) and the initial weight (ω_{0i}, ω_{1i}) of PMMA via side-chain and main-chain scissions during digestion were depicted in Eqs. 4 and 5, respectively.

$$\omega_0 = \omega_{0\mathrm{i}} - k_0 t \tag{4}$$

$$\omega_1 = \omega_{1\mathrm{i}} \exp(-k_1 t) \tag{5}$$

As the total weight of virgin PMMA (ω_t) was fixed (0.1 g) in the close digestion vessel, the Φ fraction of virgin PMMA was considered to decompose via the main-chain scission [i.e., $\omega_{1i} = \Phi\omega_t$] and the remaining fraction (1−Φ) was decomposed by the side-chain scission [i.e. $\omega_{0i} = (1-\Phi)\omega_t$]. The relationship between the remaining weight of PMMA (ω_r) and the digestion time was thus described by Eqs. 6 and 7, where the factors Φ, k_0 and k_1 were ≥ 0.[52]

$$\begin{aligned}\omega_\mathrm{r} &= \omega_0 + \omega_1 \\ &= [(1-\Phi)\cdot\omega_\mathrm{t} - k_0 t] + \Phi\cdot\omega_\mathrm{t}\exp(-k_1 t)\end{aligned} \tag{6}$$

$$\omega_\mathrm{r}(\%) = 100\frac{\omega_\mathrm{r}}{\omega_\mathrm{t}} = 100\left[(1-\Phi) - \frac{k_0 t}{\omega_\mathrm{t}}\right] + \Phi\cdot\exp(-k_1 t) \tag{7}$$

The Newton's method is often used to solve nonlinear equations by iterative approximation to minimize the square sum of deviations between experimental and modeled data. To obtain the values of Φ, k_0 and k_1 at different temperatures, the Newton's method was utilized to fit the modeled values governed by Eq. 7 to the experimental data. By introducing the values of Φ, k_0 and k_1 listed in Table 2 into Eq. 7, the relationship between the experimental and the modeled results at various temperatures were obtained as shown in Figure 5. According to the coefficients of determination (0.904–0.991), the proposed model fitted very well to the experimental data. The R^2 value (0.904) derived from the model fitting (the zero- and first-order combined kinetics) at 423 K was very similar to that of the simple zero-order kinetics ($R^2 = 0.904$). Nevertheless, the fitting at 433 K by this model was much better ($R^2 = 0.970$) than that by simple zero-order kinetics ($R^2 = 0.518$). Furthermore, according to the Φ values (Table 2), the first-order reaction ($\Phi = 0.63$) dominated at the higher temperatures (453 K and 473 K), while the zero-order reaction ($\Phi \leq 0.15$) dominated at the lower temperature (423–443 K). This conformed to the results exhibited in Figure 4. Orders other than the zero and the first were also introduced to replace x and y in Eq. 2 to carry out similar fittings. However, poor R^2 values were obtained, which invalidated the derived models.

To estimate the activation energy (E_a) of the decomposition (the required threshold energy to induce decomposition by a collision), the Arrhenius equation [Eq. 8][53] was utilized. The k_i ($i = 0$ or 1) and A denoted the rate constant and pre-exponential factor respectively, which corresponded to the frequency of collisions or the entropy.[54] Here, A was temperature-dependent but not strictly a constant[55]; R symbolized

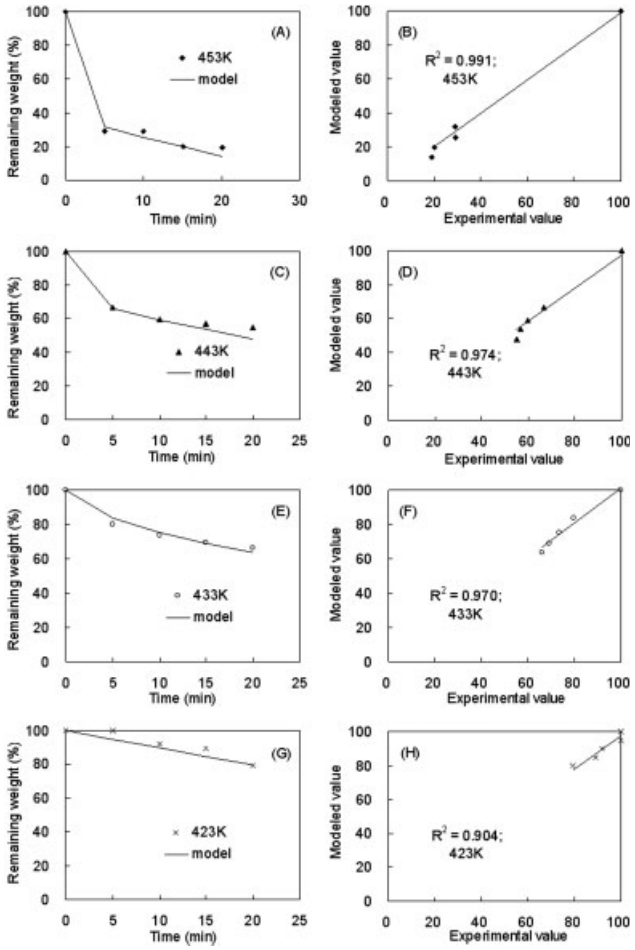

Figure 5. (A–H) Consistency between the experimental and the modeled values of the remaining weight of PMMA after microwave digestion with 3 mL of HNO_3 at the tested temperatures.

the universal gas constant (8.314 J/mole/K). In Eq. 8, the A and E_a factors were regarded as independent of temperature [T (in Kelvin)] when $E_a \gg RT$.

$$k_i(T) = A \exp\left(\frac{-E_a}{RT}\right) \tag{8}$$

By taking natural logarithms of both sides, this equation was manipulated into a linear form as illustrated in Eq. 9.

$$\ln k_i(T) = \ln A - \frac{E_a}{R}\left(\frac{1}{T}\right) \tag{9}$$

A reasonably straight line was obtained by plotting the rate constant in natural logarithm ($\ln k_i$) against the reciprocal temperature ($1/T$). According to Eq. 9, the slope corresponded to $-E_a/R$, while the intercept with the vertical axis at $1/T = 0$ was $\ln A$. The rate constants of the zero- and first-order reactions were then introduced into Eq. 9 to determine the activation energy. The obtained slopes ($-E_a/R$) of the two regression lines were -899.87 and -14691 with R^2 values of 0.931 and 0.995, respectively. Thus, the activation energies for the zero- and first-order reactions were further estimated as 7.49 and 122 kJ/mole, and the A factors were 8.50×10^{-3} g/min and 3.80×10^{14} min^{-1}, respectively. However, the E_a/RT ratios were 1.98–2.12 and 32.4–34.7, respectively, for the zero- and first-order reactions, which conflicted with the requirement of $E_a \gg RT$ for the temperature-independent assumption of E_a and A. To follow the general definition of E_a for any rate process applicable whether or not E_a depended on T,[56] Eq. 10 was developed by modifying Eq. 8.

$$E_a \equiv RT^2 \frac{d \ln k}{dT} \tag{10}$$

From the diagram of lnk versus $1/T$, as shown in Figure 6, a good linearity existed and thus the slope, $d\ln k/dT$, was identical to the value of $\Delta\ln k/\Delta T$ as a constant. Furthermore, respective activation energies (E_0 and E_1) of the zero-order and first-order reactions were then calculated from the slopes of the linear regression lines, as listed in Table 3. In addition, the A factors (A_0 and A_1 respectively for the zero- and first-order reactions; Table 3) were estimated respectively from the intercept in Eq. 10. The activation energies were 6.98–8.01 kJ/mol (mean value = 7.49 kJ/mol) for the zero-order reactions, while those for the first-order reactions were 114–130 kJ/mol (mean value = 122 kJ/mol). Since the activation energy for the first-order reaction was about an order higher than that for the zero-order reaction, the former was suggested to be more susceptible to temperature variation, according to Eq. 10. The A factors for the zero- and first-order reactions were estimated to be 7.23×10^{-3}–9.67×10^{-3} g/min and 1.15×10^{13}–1.12×10^{15} min^{-1}, respectively. As illustrated in Figure 6, the rate constants of weight loss for the first-order reaction apparently depended on the digestion temperature, while those for the zero-order reaction showed less dependence on the temperature. The increase of

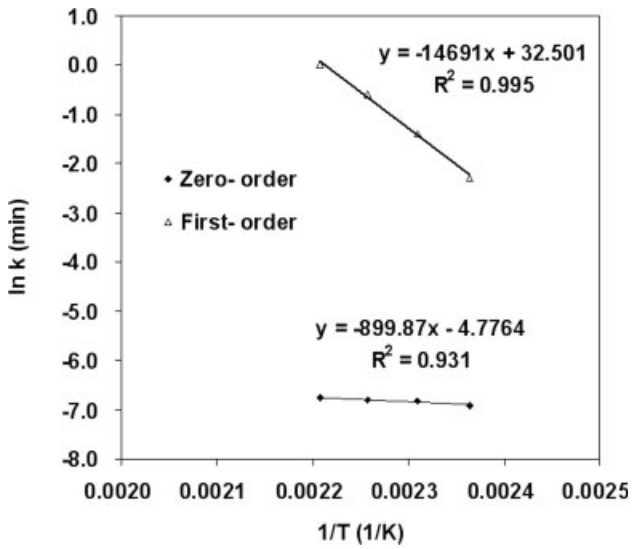

Figure 6. Relationships between the digestion temperature and the rate constants for PMMA decomposition via the zero- and first-order kinetics during microwave/HNO_3 (3 mL) digestion.

Table 3. Activation Energies and the Pre-Exponential Factors at Various Temperatures for PMMA Decomposition in 3 mL of Concentrated HNO_3 Using Microwave Irradiation

Digestion temperature (K)	E_0* (kJ/mol)	E_1† (kJ/mol)	A_0‡ (g/min)	A_1§ (min^{-1})
453	8.01	130	9.67×10^{-3}	1.12×10^{15}
443	7.66	125	8.82×10^{-3}	2.93×10^{14}
433	7.32	119	8.27×10^{-3}	6.08×10^{13}
423	6.98	114	7.23×10^{-3}	1.15×10^{13}

*Activation energy for the zero-order reaction.
†Activation energy for the first-order reaction.
‡Pre-exponential factor for the zero-order reaction.
§Pre-exponential factor for the first-order reaction.

reaction order with the temperature was ascribed to the increase of effective collisions (i.e., collisions whose energy exceeded the activation energy), vibrational energy of PMMA, and the multiplication of reacting surface area due to the fragmentation of PMMA.

Figure 7 illustrates the effect of HNO_3 volume on PMMA decomposition with 5 min of digestion time. At 423 and 443 K, the remaining weight of PMMA declined with increasing HNO_3 volume. The HNO_3 apparently enhanced the digestion efficiency as the added volume was increased to more than 3 mL. The increase of digestion efficiency was attributed to the increase of oxidizing potential of HNO_3. As the volume of HNO_3 was increased to more than 3 mL at 473 K, the digestion efficiency for PMMA increased to almost 100%. At this temperature, the effect of HNO_3 volume on digestion efficiency became insignificant when the HNO_3 volume was more than 5 mL.

As the rate constants in this work depended only on temperature, the effect of HNO_3 volume should be corresponding to the fraction (Φ) of PMMA decomposed by the main-chain scission, as shown in Eq. 7. By introducing the digestion time (i.e., $t = 5$), the digestion efficiencies and the rate constants at different temperatures into Eq. 7, the Φ values were determined (Table 4) using Newton's method. The Φ values increased with HNO_3 volume at 423 and 443 K, but the values varied insignificantly at 453 and 473 K, as illustrated in Figure 8.

Table 4. Predicted Φ Values at Various HNO_3 Volumes and Digestion Temperatures with 5 min of Digestion Time

Digestion temperature (K)	HNO_3 (mL)			
	2	3	5	7
423	5.00×10^{-3}	5.00×10^{-3}	8.00×10^{-2}	1.30×10^{-1}
443	1.50×10^{-1}	3.00×10^{-1}	4.50×10^{-1}	5.00×10^{-1}
453	6.25×10^{-1}	6.30×10^{-1}	6.70×10^{-1}	7.50×10^{-1}
473	8.90×10^{-1}	9.10×10^{-1}	9.26×10^{-1}	9.26×10^{-1}

Conclusions

The results of this study provided a new method for recycling PMMA (120,000 g/mol) economically as well as proposed a bi-order kinetic model for the decomposition of PMMA by microwave/HNO_3 digestion. Based on the experimental results and the proposed model, the following findings were established from this study. The PMMA polymer became hydrophilic due to hydrolysis after digestion by microwave irradiation in concentrated HNO_3 solution. The dominant products were volatile monomers, such as MMA and hydrophilic compounds with —COOH groups. As the digestion temperature increased, the surface area of the PMMA material enlarged while its particle size decreased and the size distribution narrowed. The PMMA decomposition was proposed and validated following a bi-order kinetics

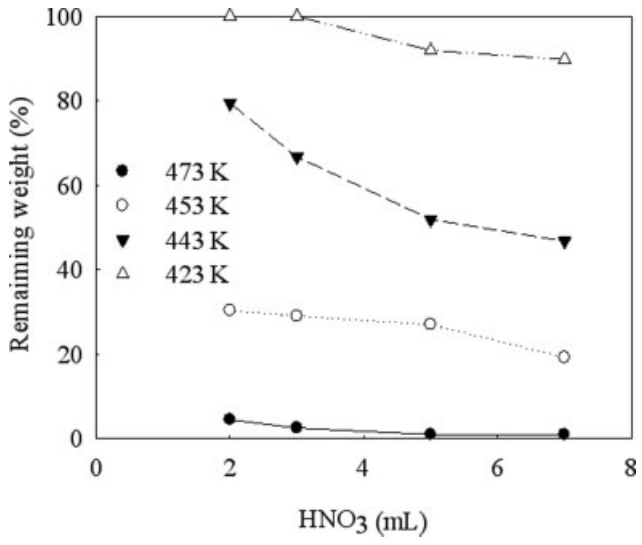

Figure 7. Variation of remaining weight of PMMA with the HNO_3 volume at digestion temperatures of 423 K, 443 K, 453 K, and 473 K.

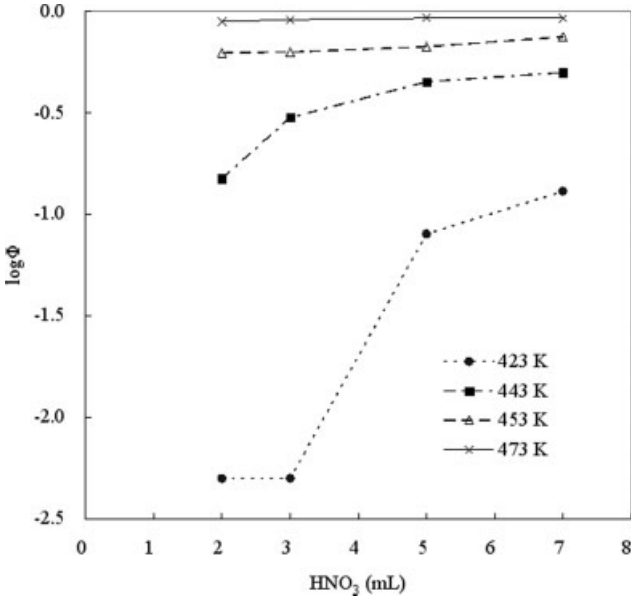

Figure 8. Predicted Φ values for PMMA decomposition by microwave digestion with 2–7 mL of HNO_3 at different tested temperatures.

model, which combined the main-chain scissions via first-order kinetics with the side-chain scissions via zero-order kinetics. The kinetic model was well fitted to experimental data for the remaining weight of PMMA after microwave/HNO_3 digestion under the tested temperatures. The first-order reaction dominated at high temperatures (453 K and 473 K), while the zero-order reaction dominated at the lower temperature range (423–443 K). Moreover, the digestion efficiency for PMMA was obviously enhanced at lower temperature (423 and 443 K) and increased to almost 100% at 473 K when HNO_3 volume was more than 3 mL, which was ascribed to the oxidizing potential increase of HNO_3. The Φ values also increased with HNO_3 volume at 423 and 443 K. However, at 453 and 473 K, the variation of Φ values was insignificant.

Acknowledgements

The LC-RID, GC-MS and GPC analysis assisted by Dr. Wei-Hsi Chen at Cellulosic Bioethanol project of INER, technical assistance from Mr. Hwa-Chou Wei as well as writing suggestion from Dr. How-Chiun Wu and Dr. Li-June Ming was deeply appreciated.

Literature Cited

1. Arisawa H, Brill TB. Kinetics and mechanisms of flash pyrolysis of poly (methyl methacrylate) (PMMA). *Combust Flame*. 1997;109: 415–426.
2. Sarantopoulou E, Kollia Z, Cefalas AC, Manoli K, Sanopoulou M, Goustouridis D, Chatzandroulis S, Raptis I. Surface nano/micro functionalization of PMMA thin films by 157 nm irradiation for sensing applications. *Appl Surf Sci*. 2008;254:1710–1719.
3. Zeng WR, Li SF, Chow WK. Study of the combustion mechanism of poly (methyl methacrylate). *Polym Mater Sci Eng Chin Ed*. 2003;19:183–186.
4. Nakajima M, Yoshikawa T, Sogo K, Hirai Y. Fabrication of multi-layered nano-channels by reversal imprint lithography. *Microchem J*. 2006;83:876–879.
5. Reddy MS, Kurose K, Okuda T, Nishijima W, Okada M. Separation of polyvinyl chloride (PVC) from automobile shredder residue (ASR) by froth flotation with ozonation. *J Hazard Mater*. 2007; 147:1051–1055.
6. Jacobsen NL, Mitchell DL, Johnson DL, Holt RA. Lased and sand-blasted denture base surface preparations affecting resilient liner bonding. *J Prosthet Dent*. 1997;78:153–158.
7. Taguenang JM, Kassu A, Ruffin PB, Brantley C, Edwards E, Sharma A. Reversible UV degradation of PMMA plastic optical fibers. *Opt Commun*. 2008;281:2089–2092.
8. Singh HP, Kumar R, Sekhon SS. Correlation between ionic conductivity and fluidity of polymer gel electrolytes containing $NH_4CF_3SO_3$. *Bull Mat Sci*. 2005;28:467–472.
9. Reiter J, Vondrák J, Mička Z. Solid-state Cd/Cd^{2+} reference electrode based on PMMA gel electrolytes. *Solid State Ion*. 2007;177: 3501–3506.
10. Krejza O, Velická J, Sedlaříková M, Vondrák J. 2008. The presence of nanostructured Al_2O_3 in PMMA-based gel electrolytes. *Macromol Mater Eng*. 2008;178:774–778.
11. Yang H, Huang M, Wu J, Lan Z, Hao S, Lin J. The polymer gel electrolyte based on poly(methyl methacrylate) and its application in quasi-solid-state dye-sensitized solar cells. *Mater Chem Phys*. 2008;110:38–42.
12. Denq BL, Hu YS, Chiu WY, Chen LW, Chiu YS. Thermal degradation behavior and physical properties for poly(methyl methacrylate) blended with propyl ester phosphazene. *Polym Degrad Stab*. 1997;57:269–278.
13. Su L, Hong Q, Lu Z. All solid-state electrochromic window of Prussian Blue and electrodeposited WO_3 film with PMMA gel electrolyte. *J Mater Chem*. 1998;8:85–88.
14. PlasticsEurope(Association of Plastics Manufacturers). Available at:http://www.plasticseurope.org.
15. MarketResearches and Consulting, Ltd. Available at:http://mcgroup.co.uk/researches/P/171/Polymethyl%20Methacrylate%20(Organic%20Glass) 20Market%20Research.html.
16. McCoy BJ, Madras G. Discrete and continuous models for polymerization and depolymerization. *Chem Eng Sci*. 2001;56:2831–2836.
17. Kang BS, Kim SG, Kim JS. Thermal degradation of poly(methyl methacrylate) polymers: kinetics and recovery of monomers using a fluidized bed reactor. *J Anal Appl Pyrolysis*. 2008;81:7–13.
18. Fordham PJ, Gramshaw JW, Castle L, Crews HM, Thompson D, Parry SJ, McCurdy E. Determination of trace elements in food contact polymers by semi-quantitative inductively coupled plasma mass spectrometry. Performance evaluation using alternative multi-element techniques and in-house polymer reference materials. *J Anal At Spectrom*. 1995;10:303–309.
19. Merten D, Broekaert JAC, Brandt R, Jakubowski N. Analysis of ZrO_2 powders by microwave assisted digestion at high pressure and ICP atomic spectrometry. *J Anal At Spectrom*. 1999;14:1093–1098.
20. Sun YC, Ko CJ. Evaluation of closed-vessel microwave digestion method for the determination of trace impurities in polymer-based photoresist by inductively coupled plasma mass spectrometry. *Microchem J*. 2004;78:163–166.
21. Kosmidis VA, Achilias DS, Karayannidis GP. PET recycling and recovery of pure terephthalic acid. *Macromol Mater Eng*. 2001: 286:640–647.
22. Holland BJ, Hay JN. The effect of polymerisation conditions on the kinetics and mechanisms of thermal degradation of PMMA. *Polym Degrad Stab*. 2002;77:435–439.
23. Coltelli MB, Bianchi S, Aglietto M. Poly(ethylene terephthalate) (PET) degradation during the Zn catalysed transesterification with dibutyl maleate functionalized polyolefins. *Polymer*. 2007;48: 1276–1286.
24. Kaminsky W, Zorriqueta IJN. Catalytical and thermal pyrolysis of polyolefins. *J Anal Appl Pyrolysis*. 2007;79:368–374.
25. Dubreuil MF, Bongaers EM. Use of atmospheric pressure plasma technology for durable hydrophilicity enhancement of polymeric substrates. *Surf Coating Tech*. 2008;202:5036–5042.
26. Mitan NMM, Bhaskar T, Hall WJ, Muto A, Williams PTY, Sakata. Effect of decabromodiphenyl ether and antimony trioxide on controlled pyrolysis of high-impact polystyrene mixed with polyolefins. *Chemosphere*. 2008;72:1073–1079.
27. Wondraczek K, Adams J, Fuhrmann J. Change of tacticity during thermal degradation of PMMA. *Macromol Chem Phys*. 2002;203: 2624–2629.
28. Ferriol M, Gentilhomme A, Cochez M, Oget N, Mieloszynski JL. Thermal degradation of poly(methyl methacrylate) (PMMA): modelling of DTG and TG curves. *Polym Degrad Stab*. 2003;79:271–281.
29. Kathryn JL, Steve JH. Microwave digestion procedures for environmental matrices. Critical review. *Analyst*. 1998;123:103R–133R.
30. Liu J, Harris AT. Microwave-assisted acid digestion of alumina-supported carbon nanotubes. *Sep Purif Technol*. 2008;62:602–608.
31. Marimuthu A, Madras G. Continuous distribution kinetics for microwave-assisted oxidative degradation of poly(alkyl methacrylates). *AIChE J*. 2008;54:2164–2173.
32. Michel H, Levent D, Barci V, Barci-Funel G, Hurel C. Soil and sediment sample analysis for the sequential determination of natural and anthropogenic radionuclides. *Talanta*. 2008;74:1527–1533.
33. Epov VN, Benkhedda K, Evans RD. Determination of Pu isotopes in vegetation using a new on-line FI-ICP-DRC-MS protocol after microwave digestion. *J Anal At Spectrom*. 2005;20:990–992.
34. Mesko MF, Moraes DP, Barin JS, Dressler VL, Knapp G, Flores EMM. Digestion of biological materials using the microwave-assisted sample combustion technique. *Microchemical J*. 2006;82: 183–188.
35. Madras G, Smith JM, McCoy BJ. Degradation of poly (methyl methacrylate) in solution. *Ind Eng Chem Res*. 1996;35:1795–2074.
36. Costache MC, Wang D, Heidecker MJ, Manias E, Wilkie CA. The thermal degradation of poly (methyl methacrylate) nanocomposites with Montmorillonite, layered doubled hydroxides and carbon nanotubes. *Polym Adv Technol*. 2006;17:272–280.
37. Holland BJ, Hay JN. The kinetics and mechanisms of the thermal degradation of poly (methyl methacrylate) studied by thermal analysis-Fourier Transform Infrared Spectroscopy. *Polymer*. 2001;42: 4825–4835.

38. Madras G, Karmore V. Continuous distribution kinetics for oxidative degradation of PMMA in Solution. *Polym Degrad Stab*. 2001;72: 537–541.
39. Gao Z, Kaneko T, Hou D, Nakada M. Kinetics of thermal degradation of poly (methyl methacrylate) studied with the assistance of the fractional conversion at the maximum reaction rate. *Polym Degrad Stab*. 2004;84:399–403.
40. Achilias DS. Chemical recycling of poly(methyl methacrylate) by pyrolysis. Potential use of the liquid fraction as a raw material for the reproduction of the polymer. *Eur Polymer J*. 2007;43:2564–2575.
41. Zeng WR, Li SF, Chow WK. The kinetic study of PMMA isothermal combustion. *Chin J Chem Phys*. 2003;16:317–320.
42. Zeng WR, Li SF, Chow WK. Chemical kinetics on thermal oxidative degradation of PMMA. *Chin J Chem Phys*. 2003;16:64–68.
43. Denq BL, Chiu WY, Lin KF. Kinetic model of thermal degradation of polymers for nonisothermal process. *J Appl Polym Sci*. 1997; 66:1855–1868.
44. Stoliarov SI, Westmoreland PR, Nyden MR, Forney GP. A reactive molecular dynamics model of thermal decomposition in polymers. I. Poly (methyl methacrylate). *Polymer*. 2003;44:883–894.
45. Chang YC, Chu TC. Research on nano-material synthesis, self-assembling and decomposition mechanism with microwave heating technology, M.Sc. Thesis, National Tsing-Hua University, Taiwan, Republic of China, July 2003:92–94.
46. Levine IN. *Physical Chemistry*. Singapore: McGraw-Hill, 1988: 438–439.
47. Brady JE, Sense F. *Chemistry*. New York: Wiley, 2004:439.
48. Levine IN. *Physical Chemistry*. Singapore: McGraw-Hill, 1988;524: 576.
49. Levine IN. *Physical Chemistry*. Singapore: McGraw-Hill, 1988:516.
50. Baumgaertel A, Becer CR, Gottschaldt M, Schubert US. MALDI-TOF MS coupled with collision-induced dissociation (CID) measurements of poly(methyl methacrylate). *Macromol Rapid Commun*. 2008;29:1309–1315.
51. Manring LE. Thermal degradation of poly(methyl methacrylate). 4. Random side group scission. *Macromolecules*. 1991;24:3304–3309.
52. Saastad OW, Uggerud E. Simulation of the kinetics of a chemical system as a method for determination of rate constants from experimental data. *Phys Scr*. 1991;T38:88–90.
53. Brauner N, Shacham M. Statistical analysis of linear and nonlinear correlation of the Arrhenius equation constants. *Chem Eng Process*. 1997;36:243–249.
54. Schwaab M, Pinto JC. Optimum reference temperature for reparameterization of the Arrhenius equation. Part 1: Problems involving one kinetic constant. *Chem Eng Sci*. 2007;62:2750–2764.
55. Turn SR. *An Introduction to Combustion: Concepts and Applications*. New York: McGraw-Hill, 1994:127.
56. Levine IN. *Physical Chemistry*. Singapore: McGraw-Hill, 1988:539.

Manuscript received Aug. 27, 2008, and revision received Dec. 16, 2008.